Bacteria Viability in Sol−Gel Materials Revisited: Cryo-SEM as a Suitable Tool To Study the Structural Integrity of Encapsulated Bacteria

Maria L. Ferrer,[†] Zaira Y. Garcia-Carvajal,[†] Luis Yuste,[‡] Fernando Rojo,[‡] and Francisco del Monte*,[†]

Instituto de Ciencia de Materiales de Madrid (ICMM) and Centro Nacional de Biotecnología (CNB), Consejo Superior de Investigaciones Científicas (CSIC), Campus de Cantoblanco, 28029 Madrid, Spain

Received October 7, 2005

Biocompatibility is an important issue that still needs research if one desires to fully preserve the metabolic activity of cells encapsulated in any type of material. Spectroscopic techniques (e.g., NMR and fluorescence) have been used to study the viability decrease upon aging time of bacteria encapsulated in silica gel materials. Unfortunately, none of these spectroscopic techniques are able to provide insights about the detrimental causes affecting the viability of encapsulated cells. The current work uses cryo-scanning electron microscopy (cryo-SEM) for the in situ study of hydrated biocomposites, given its ability for mapping the water distribution within the host matrix. Cryo-SEM is accompanied by fluorescence experiments which allow correlating the metabolic activity of the cells with their structural integrity. The combination of these techniques provides useful information for the design of new biocomposites where encapsulated bacteria preserve their structural integrity and, thus, are viable for periods of time in a range similar to those found for bacteria suspended in buffered solutions.

Introduction

Since 1990[1] and for more than a decade,[2] sol−gel preparation of different biocomposites has been the objective of numerous research groups. More recently, research has focused on the development of sol−gel biocomposites capable of being applied in many different fields, from biosensing to biocatalysis up to biomedicine.[3] A very interesting application recently developed is based on the use of sol−gel surfaces as solid supports for cell growth (two-dimensional (2D) cultures), an approach useful for both simple organisms such as bacteria and the more complex and demanding mammalian cells.[4] However, it is in many cases necessary to grow cells in three-dimensional (3D) structures (3D cultures), rather than in surfaces, because only a 3D culture can mimic in vivo growth conditions where the mechanical and biochemical interplay between cells and the surrounding extracellular matrix are rather complex.[5] For example, the transformation of cancerous breast cells into noncancerous ones through the use of a determined therapy has been observed in 3D but not in 2D cultures.[6] To date, the material of choice as a 3D support for cell growth has been basically restricted to several polymer foams and scaffolds, which have been demonstrated to have a structure and a biocompatibility that allows colonization by different living cells.[7]

The sol−gel preparation of biocompatible and porous 3D supports where cells might proliferate within the confined porosity is of great interest. From a structural point of view, and to allow for cells proliferation, porous materials should be adjusted in terms of cavity size for every particular case; that is, the cell size ranges from a few micrometers for most bacteria to about 100 μm for animal cells.[8] Different sol−gel approaches have demonstrated their ability in the preparation of foams and scaffolds with tuned macroporous structures.[9] Unfortunately, preliminary results on cell growth obtained with sol−gel based materials[10] are still far from those

* Corresponding author. Fax: +34 91 372 0623. E-mail: delmonte@icmm.csic.es.

[†] Instituto de Ciencia de Materiales de Madrid.

[‡] Centro Nacional de Biotecnología.

(1) Braun, S.; Rappoport, S.; Zusman, R.; Avnir, D.; Ottolenghi, M. *Mater. Lett.* **1990**, *10*, 1.

(2) Among others: (a) Avnir, D.; Braun, S.; Lev, O.; Ottolenghi, M. *Chem. Mater.* **1994**, *6*, 1605. (b) Ellerby, L. M.; Nishida, C. R.; Nishida, F.; Yamanaka, S. A.; Dunn, B.; Valentine, J. S.; Zink, J. I. *Science* **1992**, *255*, 1113. (c) Lan, E. H.; Dave, B. C.; Fukuto, J. M.; Dunn, B.; Zink, J. I.; Valentine, J. S. *J. Mater. Chem.* **1999**, *9*, 45. (d) Das, T. K.; Khan, I.; Rousseau, D. L.; Friedman, J. M. *J. Am. Chem. Soc.* **1998**, *120*, 10268. (e) Badjiæ, J. D.; Kostiæ, N. M. *Chem. Mater.* **1999**, *11*, 3671. (f) Bhathia, R. B.; Brinker, C. F.; Gupta, A. K.; Singh, A. K. *Chem. Mater.* **2000**, *12*, 2434. (g) Gill, I.; Ballesteros, A. *J. Am. Chem. Soc.* **1998**, *120*, 8587.

(3) (a) Besanger, T.; Easwaramoorthy, B.; Brennan, J. D. *Anal. Chem.* **2004**, *76*, 6470. (b) Luo, T.-J. M.; Soong, R.; Lan, E.; Dunn, B.; Montemagno, C. *Nat. Mater.* **2005**, *4*, 220. (c) Roth, K. M.; Zhou, Y.; Yang, W.; Morse, D. E. *J. Am. Chem. Soc.* **2005**, *127*, 325. (d) Hodgson, R. J.; Chen, Y.; Zhang, Z.; Tleugabulova, D.; Long, H.; Zhao, X.; Organ, M.; Brook, M. A.; Brennan, J. D. *Anal. Chem.* **2004**, *76*, 2780. (e) Matys, S.; Raff, J.; Soltmann, U.; Selenska-Pobell, S.; Böttcher, H.; Pompe, W. *Chem. Mater.* **2004**, *16*, 5549.

(4) (a) Armon, R.; Starosvetzky, J.; Saad, I. *J. Sol-Gel Sci. Technol.* **2000**, *19*, 289. (b) Perlata-Perez, M. R.; Saucedo-Castaneda, G.; Gutierrez-Rojas, M. *J. Sol-Gel Sci. Technol.* **2001**, *20*, 105. (c) Zolkov, C.; Avnir, D.; Armon, R. *J. Mater. Chem.* **2004**, *14*, 2200.

(5) (a) Ryadnov, M. G.; Woolfson, D. N. *Nat. Mater.* **2003**, *2*, 329. (b) Richardson, T. P.; Peters, M. C.; Ennett, A. B.; Mooney, D. J. *Nat. Biotechnol.* **2001**, *19*, 1029. (c) Lutolf, M. P.; Lauer-Fields, J. L.; Schmoekel, H. G.; Metters, A. T.; Weber, F. E.; Fields, G. B.; Hubbell, J. A. *Proc. Natl. Acad. Sci. U.S.A.* **2003**, *100*, 5413.

(6) (a) Wang, F.; Weaver, V. M.; Petersen, O. W.; Larabell, C. A.; Dedhar, S.; Briand, P.; Lupu, R.; Bissell, M. J. *Proc. Natl. Acad. Sci. U.S.A.* **1998**, *95*, 14821. (b) Overall, C. M.; López-Otín, C. *Nat. Rev. Cancer* **2002**, *2*, 657. (c) Sahai, E.; Marshall, C. J. *Nat. Cell Biol.* **2003**, *5*, 711.

(7) (a) Akay, G.; Erhan, E.; Keskinler, B. *Biotechnol. Bioeng.* **2005**, *90*, 180. (b) Yang, J.; Webb, A. R.; Ameer, G. A. *Adv. Mater.* **2004**, *16*, 511. (c) Barbetta, A.; Dentini, M.; De Vecchis, M. S.; Filippini, P.; Formisano, G.; Caiazza. S. *Adv. Funct. Mater.* **2005**, *15*, 118. (d) Stachowiak, A. N.; Bershteyn, A.; Tzatzalos, E.; Irvine, D. J. *Adv. Mater.* **2005**, *17* (4), 399. (e) Shea, L. D.; Smiley, E.; Bonadio, J.; Mooney, D. J. *Nat. Biotechnol.* **1999**, *17*, 551.

10.1021/cm0522275 CCC: $33.50
Published on Web 02/14/2006

with polymers[7d] no matter what identical macrostructure is used in both works (e.g., inverse opals). Surface modification of the sol−gel scaffold with bioactive components is recommended by Kotov and co-workers to further improve their biocompatibility.[10] The partial success of sol−gel materials as host matrixes for 3D cultures[10] reveals that preserving bacteria viability upon encapsulation is intrinsically more complex than upon immobilization on substrates for 2D cultures.[4c]

Thus, host matrix biocompatibility is a capital issue in sol−gel materials that still needs research if one desires to fully preserve the metabolic activity of encapsulated cells. Use of aqueous sol−gel routes has succeeded for a full preservation of the integrity of the cell membrane during the encapsulation process.[11] However, right after gelation and during the aging process, further methanol release from non-hydrolyzed alkoxides, cell exposure to chemical groups situated at the porous surface (e.g., silanol groups), and/or physical constraint exerted on the cells by the characteristic shrinkage of the matrix result in poor viability of encapsulated cells. Actually, NMR and fluorescence studies have shown that cell activity dramatically decreases up to negligible levels in just a few days after encapsulation.[11b,c] Unfortunately, neither NMR nor fluorescence spectroscopy can provide accurate data regarding the causes behind the loss of cell metabolic activity.

The current work attempts to get insights regarding the factors governing the viability of encapsulated living cells. The samples under study are hydrated silica gel materials containing *Escherichia coli* cells and stored at 4 °C in buffered solutions. The *E. coli* strain used was genetically engineered to express a fluorescent protein (green fluorescent protein, GFP) in response to the presence of medium-chain-length alkanes (C_6 to C_{11} alkanes) or of dicyclopropyl ketone (DCPK). The capability of the engineered bacteria *E. coli*-GFP to fluoresce can be used to study both the biocompatibility of the encapsulation route and the viability of encapsulated cells with aging time. However, as mentioned above, spectroscopic techniques cannot reveal the reasons for viability loss. Thus, the use of a different analytical tool is required to study the structural integrity of the encapsulated bacteria. Regardless of the nonextended use of cryo-scanning electron microscopy (cryo-SEM) in materials science,[12] it is a common tool used in biology when the preservation of the structural integrity of many different hydrated systems is required.[13] Cryo-SEM has provided insights on the water distribution within the host matrix and, ultimately, has allowed for the observation of the cell integrity when the cells are encapsulated under different conditions and after different aging times. The observation of encapsulated bacteria has guided us in the design of new host matrixes. Fluorescence spectroscopy has revealed the improved biocompatible character of such matrixes.

Experimental Section

Materials. Tetraethyl orthosilicate (TEOS), aminopropyltriethoxysilane (APTES), tris(hydroxymethyl)aminomethane (Tris), glycidyl isopropyl ether (GIE), sodium citrate, and D-gluconolactone were from Sigma-Aldrich Co. The synthesis of *N*-(3-triethoxysilylpropyl)gluconamide (GLTES) from APTES and D-gluconolactone was performed as described elsewhere.[14] The bacterial strain *E. coli*-GFP was prepared as described elsewhere.[11c] Water was distilled and deionized.

Sample Preparation. A silica sol stock solution (1 mL) is obtained by mixing 0.76 mL of TEOS, 0.24 mL of H_2O, and 5.0 μL of HCl (0.6 M). The sol is vigorously stirred for 30 min. The resulting sol is 13.6 M in EtOH given that alcohol is a byproduct of the hydrolysis reaction. For the achievement of an alcohol-free sol, rotavapor methods were applied on the hydrolyzed and diluted sol (1 mL of H_2O is added to 1 mL of sol).[11c,15] Sols containing glycerol were prepared by addition of 1 mL of a glycerol/water solution (10 wt % in glycerol), while highly diluted aqueous sols were obtained by addition of 4 mL of H_2O to 1 mL of sol. In every case, addition occurs prior to rotaevaporation. The organically modified silica sol stock solution (1 mL) is obtained by dissolving 0.135 g of GLTES in 5 μL of HCl (0.6 M) and water. The resulting sol is vigorously stirred for 30 min and submitted to rotaevaporation for alcohol removal.

TEOS based biocomposites are obtained by mixing an equal volume (75 μL) of the hydrolyzed sol and of the bacterial suspension in a cylindrical polystyrene container. GLTES/TEOS based biocomposites are obtained by mixing 52.5 μL of TEOS stock sol, 52.5 μL of GLTES stock sol, 5.0 μL of buffered solution (e.g., 1 M Tris/HCl, pH 7.5), and 75.0 μL of bacterial suspension. The TEOS/GLTES molar ratio used for biocomposites preparation is 90/10 (∼3.8 wt % of GLTES).

In both cases, gelation occurred after mixing in just a few minutes and the resulting gels are allowed to dry for 20 min at 8 °C prior to their storage at 4 °C. Wet aging was achieved by biocomposites storage in simple fresh buffered solutions (e.g., 20 mM Tris/HCl (pH 7.5), 20 mM sodium citrate) or in fresh buffered solutions containing glycerol (10 wt %). Table 1 summarizes the samples under study and experimental conditions used for their preparation.

Cryo-SEM Experiments. Small fragments of the hydrated biocomposites are mechanically fixed onto the specimen holder of a cryotransfer system (Oxford CT1500) and plunged into subcooled liquid nitrogen. Freezing of biological entities with membrane

(8) Alberts, A.; Johnson, A.; Lewis, J.; Raff, M.; Roberts, K.; Walter, P. *Molecular Biology of the Cell*, 4th ed.; Garland Science: New York, 2002.
(9) Among others: (a) Mann, S.; Ozin, G. A. *Nature* **1996**, *382*, 313. (b) Imhof, A.; Pine, D. J. *Nature* **1997**, *389*, 948. (c) Holland, B. T.; Blanford, C. F.; Stein, A. *Science* **1998**, *281*, 538. (d) Zhang, H.; Hardy, G. C.; Rosseinsky, M. J.; Cooper, A. I. *Adv. Mater.* **2003**, *15* (1), 78. (e) Mann, S. *Angew. Chem., Int. Ed.* **2000**, *39*, 3392. (f) Chandrappa, G. T.; Steunou, N.; Livage, J. *Nature* **2002**, *416*, 702. (g) Carn, F.; Colin, A.; Achard, M.-F.; Deleuze, H.; Saadi, Z.; Backov, R. *Adv. Mater.* **2004**, *16*, 140. (h) Caruso, R. A. *Angew. Chem., Int. Ed.* **2004**, *43*, 2746. (i) Mukai, S. R.; Nishihara, H.; Tamon, H. *Chem. Commun.* **2004**, *7*, 874.
(10) Kotov, N. A.; Liu, Y.; Wang, S.; Cumming, C.; Eghtedari, M.; Vargas, G.; Motamedi, M.; Nichols, J.; Cortiella, J. *Langmuir* **2004**, *20*, 7887−92.
(11) (a) Premkumar, J. R.; Lev, O.; Rosen, R.; Belkin, S. *Adv. Mater.* **2001**, *13*, 1773. (b) Nassif, N.; Bouvet, O.; Rager, M. N.; Roux, C.; Coradin, T.; Livage, J. *Nat. Mater.* **2002**, *1*, 42. (c) Ferrer, M. L.; Yuste, L.; Rojo, F.; del Monte, F. *Chem. Mater.* **2003**, *15*, 3614. (d) Finnie, K. S.; Bartlett, J. R.; Woolfrey, L. *J. Mater. Chem.* **2000**, *10*, 1099. (e) Raff, J.; Soltmann, U.; Matys, S.; Selenska-Pobell, S.; Böttcher, H.; Pompe, W. *Chem. Mater.* **2003**, *15*, 240.
(12) (a) Okun, N. M.; Ritorto, M. D.; Anderson, T. M.; Apkarian, R. P.; Hill, C. L. *Chem. Mater.* **2004**, *16*, 2551. (b) Haridas, M. M.; Menon, A.; Goyal, N.; Chandran, S.; Bellare, J. R. *T. Indian Ceram. Soc.* **1995**, *54*, 152. (c) Wyss, H. M.; Huetter, M.; Muller, M.; Meier, L. P.; Gauckler, L. J. *J. Colloid Interface Sci.* **2002**, *248*, 340.
(13) Moor, H. *Cryotechniques in Biological Electron Microscopy*; Springer-Verlag: Berlin, 1987.
(14) Tleugabulova, D.; Zhang, Z.; Chen, Y.; Brook, M. A.; Brennan, J. D. *Langmuir* **2004**, *20*, 848.
(15) Ferrer, M. L.; del Monte, F.; Levy, D. *Chem. Mater.* **2002**, *14*, 3619.

Table 1. Summary of Biocomposites Studied in This Work and Experimental Conditions Used for Their Preparation

sample	precursor (molar ratio)	aqueous sol	mL of water/ additives[a]	aging in buffer[b]
1	TEOS (100)	no	1/none	yes
2	TEOS (100)	yes	1/none	yes
3	TEOS (100)	yes	4/none	yes
4	TEOS (100)	yes	1/glycerol	yes
5	TEOS/GLTES (90/10)[c]	yes	1/none	yes

[a] Water and additives added prior rotaevaporation. [b] Aging is always performed at 4 °C. [c] The GLTES wt % is ~3.8.

structure is not a trivial issue, because the formation of ice crystals can disrupt the cellular structure. Rapid freezing is required to avoid the formation of ice crystals and preserve the aqueous component of the cell near the vitreous state (e.g., glassy water). Glassy water is obtained by very rapid cooling (10^6 °C/s).[16] The fastest cooling rate that can be achieved by direct plunge in liquid nitrogen is around 5×10^2 °C/s.[17] The low heat capacity and thermal conductivity (latent heat) of liquid nitrogen allows for the formation of a vapor barrier around the sample (e.g., the leidenfrost effect), restricting the rate at which heat is withdraw from the sample and allowing for ice crystal formation. Lowering the pressure of liquid nitrogen allows for the formation of nitrogen slush which is able to absorb heat without increasing its own temperature (heat is used for the slush to liquid transition rather than for temperature increase), and cooling rates of 10^4 °C/s can be obtained. This cooling rate is not that used for achievement of glassy water but is enough to keep ice crystal formation to a minimum. The validity of the freezing process is provided by whether ice crystals are visible at the SEM pictures. Thus, the absence of crystals in any of the pictures showed in Figure 3 guaranties the observation of bacteria in its pristine state, and, hence, the occurrence of any type of bacteria damage must be ascribed to the encapsulation process, either before or after gelation.

The frozen specimens are transferred to a preparation unit via an air lock transfer device and cryofractured. Freeze fracture operates on the principle that a specimen that is held in place frozen in ice can be treated like a solid rigid structure and broken or fractured in various regions of the specimen. These newly fractured surfaces may run along the original surface of the bacteria but are also likely to pass through them. In our case, cross-sectioned bacilli are eventually obtained for fractures shown in Figure 3A−C,E,F.

The fractured specimens are directly transferred (via a second air lock) to the microscope cold stage, where they are etched for 2 min at −90 °C. After ice sublimation, the etched surfaces are sputter coated with gold in the preparation unit. Samples are subsequently transferred onto the cold stage of the scanning electron microscope chamber. Fractured surfaces are observed with a DSM 960 Zeiss scanning electron microscope at −135 °C under the following conditions: acceleration potential, 15 kV; working distance, 10 mm; and probe current, 5−10 nA. Energy-dispersive X-ray analysis (EDX) was performed using an Oxford instrument ISIS LINK system.

Fluorescent Confocal Microscopy. Confocal microscopy was performed with a Radiance 2100 (Bio-Rad) laser scanning system on a Zeiss Axiovert 200 microscope. For fluorescence excitation, an argon ion laser with 488-nm wavelength and an appropriate combination of beam splitter and barrier filter were used. The images were simultaneously taken in the fluorescence confocal mode (depth of focus 500 nm) as well as in the transmitted light mode of the instrument using differential interference contrast according to Nomarski. It should be noted that hundreds of cells were visualized under the confocal microscope for each condition with identical morphology. For simplicity, we consider that images represent the $x-y$ plane, while the depth in focus represents the z axis.

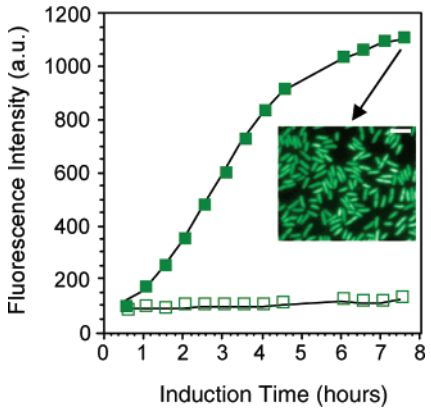

Figure 1. Fluorescence response of *E. coli*-GFP suspended in a buffered solution after addition of DCPK. (□) No DCPK added; (■) DCPK added at time 0. Inset: Fluorescent bacteria obtained after induction observed in a fluorescence microscope (bar is 4 μm).

Fluorescent Spectroscopy Experiments. Fluorescence measurements were performed in *front face* mode at 20 °C in a SLM-8000C spectrofluorimeter (SLM Instruments, Urbana, IL). The excitation wavelength was selected at 485 nm. The fluorescent spectrum of every sample was the mean of three independent experiments, performed in duplicate. Appropriate blanks were respectively subtracted to minimize the scattering contribution in the sample emission.

Results and Discussion

The metabolic activity of the bacterial cells used in this work can be determined by measuring their fluorescent response to the presence of an inducer (e.g., DCPK). The increase of the fluorescence intensity shown in Figure 1 for bacteria suspended in a buffered solution reports the cell ability to express the GFP, and the bacteria becomes strongly fluorescent (see inset of Figure 1). The first issue under study must be the tolerance of *E. coli*-GFP to the ethanol produced during TEOS hydrolysis and condensation. Figure 2A shows how the exponential growth of cells is completely disrupted for ethanol concentrations of ~2.2 M (10 wt %) and above, in the range of those previously reported for methanol.[11c] Note that the ethanol concentration at the sol resulting from TEOS hydrolysis is 12.8 M, which makes mandatory the use of alcohol-free sol−gel routes for bacteria encapsulation. Otherwise, even highly fluorescent bacteria (e.g., DCPK induced) rapidly lose intensity of fluorescence emission when suspended in a nonaqueous silica sol, most likely because of membrane lysis and subsequent cell death. Fluorescence vanishing also indicates GFP denaturation, as a consequence of protein exposure to ethanol after membrane lysis.[11c]

Comparison of cryo-SEM micrographs of bacteria encapsulated in TEOS based sol−gel materials prepared from an alcoholic sol (sample 1, Figure 3A) or an alcohol-free route (sample 2, Figure 3B) shows that the presence of alcohol results in the loss of interface between bacteria and the host matrix (arrows indicate some representative cases). However, when encapsulation proceeds in absence of alcohol (sample 2, Figure 3B) cell envelope integrity appears well-preserved (e.g., well-delimited bacteria membrane with neither evidence

(16) Mayer, E. *J. Appl. Phys.* **1985**, *58*, 663.
(17) Kirsop, B. E.; Doyle, A. *Maintenance of Microorganism and Cutltured Cells*; Academic Press: London, 1991.

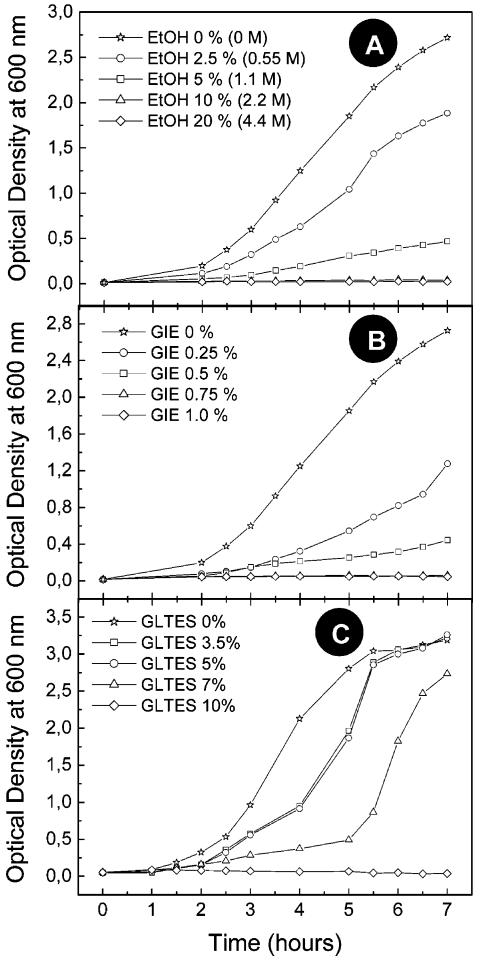

Figure 2. Exponential growth of *E. coli* cells in the presence of different compounds. Cells were grown in a complete LB medium supplemented with the inducer DCPK (0.05%) and the indicated amounts of ethanol (A), GIE (B), or GLTES (C). The graph shows the increase in culture density (A_{600}) as a function of time.

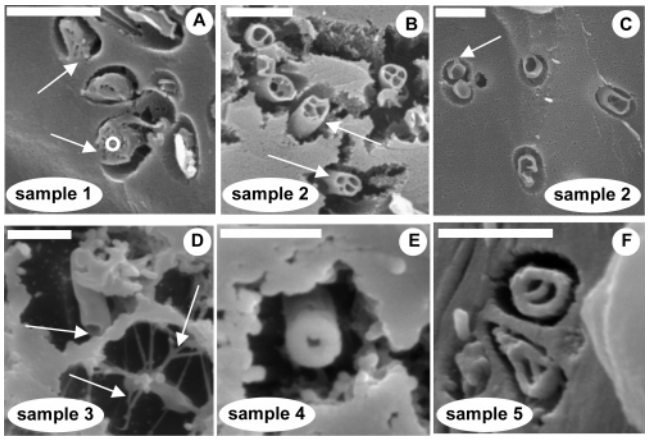

Figure 3. Cryo-SEM pictures of *E. coli*-GFP encapsulated in different silica matrixes (samples 1−5). Bacteria are visualized as cross-sectioned bacilli because of freeze fracture. Bar is 2 μm.

of lysis nor virtual adhesion to the matrix surface). In addition, a close inspection of Figure 4B shows that bacteria encapsulated through an alcohol-free route are visualized as empty cavities with thin inner hedges crossing such cavities, which most likely correspond to lyophilized compounds of the cell's cytoplasm. Bacteria encapsulated through an alcoholic sol show a different picture and look filled rather than void (Figure 3A). EDX analysis on the inner bacteria cavity

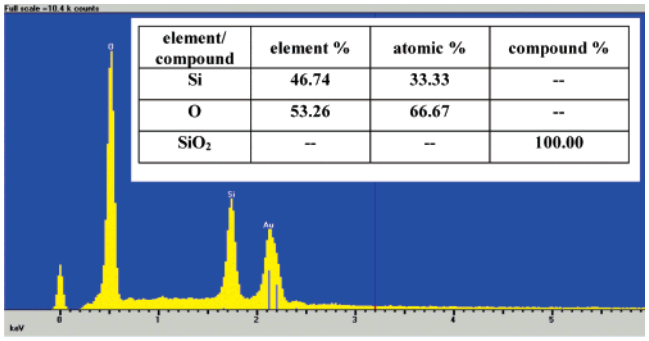

Figure 4. EDX analysis on the inner cavity of *E. coli*-GFP encapsulated through a nonaqueous sol−gel route. The white circle at Figure 3A indicates the spot where EDX analysis was performed.

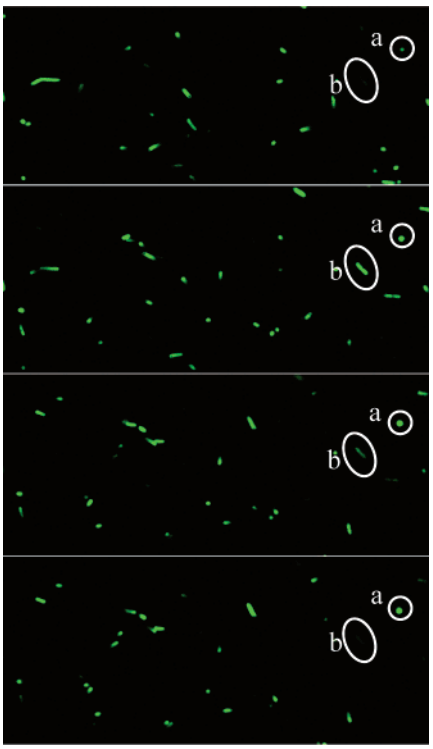

Figure 5. Confocal microscope images showing different successive layers of a silica matrix containing encapsulated *E. coli*-GFP fluorescent cells.

(Figure 4) reveals the presence of stoichiometric silica (e.g., SiO_2) but no trace of carbon (note that samples are gold metallized, and, hence, there is a peak for Au). This scenario is indicative of ethanol inducing membrane lysis at the sol stage prior to gelation so that silica gains access to the cell's interior.

Note that both images (Figure 3A,B) correspond to freeze fractured samples and cells are, therefore, visualized as cross-sectioned bacilli. Fluorescence confocal microscopy shown in Figure 5 can help to understand the occurrence of cross-sectioned bacilli upon fracture. Successive images slicing the sample depth at intervals of 0.5 μm reveals a homogeneous 3D bacteria dispersion within the silica matrix. A single cell can be visualized in just a couple of slices (b) or in up to four slices (a), depending on their orientation ($x-y$ in-plane or z-axis aligned, respectively). Thus, the single cell z-axis aligned would be visualized as cross-sectioned bacilli in an eventual freeze fracture of the sample concurring with slice 3.

Bacteria encapsulated through an alcoholic sol are unable to respond to the presence of DCPK (no fluorescent GFP produced in response to DCPK), which indicates that they are severely damaged.[11c] Cells encapsulated in TEOS based biocomposites using an alcohol-free route exhibit a good fluorescence response, in the range of that previously reported for cells encapsulated in tetramethyl orthosilicate (TMOS) based biocomposites and suspended in buffered solutions (see Supporting Information for fluorescent spectra).[11c] All this suggests that the occurrence of membrane lysis observed in the cryo-SEM images can be correlated to loss of bacteria activity.

We have previously observed that the metabolic activity of encapsulated cells vanishes in about 1 week, even if the matrix was performed by an alcohol-free route and was kept immersed in a buffered solution.[11c] Cryo-SEM micrographs of such aged matrixes (sample 2, Figure 3C) show bacteria with clear signs of cell dehydration; for example, collapsed membranes of irregular shape and absence of inner fluids. It is noteworthy that a water interface between the bacteria and the silica gel is mostly present around the cells, except in some individual locations through which bacteria links to the matrix.

Cryo-SEM micrographs shown in Figure 3A,B, together with the data on metabolic activity[11c] and on ethanol toxicity (Figure 2A), show a clear correlation between loss of viability and the presence of structural damages at the bacterial membrane. Similarly, comparison of the images shown in Figure 4B,C suggests that the loss of bacterial viability that occurs as the encapsulated bacteria age inside the host matrix might be a consequence of progressive matrix shrinkage and subsequent exposure of the cell membrane to the chemical groups of the surrounding matrix. The question that arises is whether a matrix with a very wide pore size could be capable to minimize bacteria and pore surface interactions and, hence, improve bacteria viability. To answer this question we prepared an open matrix (e.g., scaffold)[9] where the absence of physical constrain on bacteria is guaranteed. In this case, scaffolds were just obtained through further water dilution prior rotaevaporation (sample 3 in Table 1) which guaranties the biocompatibility of the preparation process. Actually, Lev and co-workers have successfully encapsulated living cells through a diluted sol−gel process without removal of alcohol.[11a] However, despite the open porous structure of the scaffold, links between cells and matrix and membrane holes are observed 4 days after encapsulation (Figure 3D). Therefore, physical constrain of the bacteria within the host matrix does not seem to be a direct cause of cell death. Rather, our results suggest that effective cell isolation from the porous surface of the silica host matrix could better contribute to a significant improvement of cell viability. However, it is worthy to mention that even if physical constraint does not directly affect cell viability in scaffolds and wet aged samples, it may play a role in long term storages and, of course, in nonwet aged samples (see Supporting Information for further details on this issue). This is the intrinsic complexity that implies encapsulation versus immobilization, given that chemical interactions are more likely to be established when bacteria are fully surrounded by the supporting host than when they are just lying on top of it.[18]

Regarding bacteria isolation from the host matrix, Livage and co-workers[11b] reported that incorporation of glycerol in the host matrixes results in viabilities for encapsulated bacteria even better than those obtained for bacteria suspended in a buffered solution. The incorporation of glycerol seems to form a chemical barrier between bacteria and the host matrix. Figure 3E indeed shows that incorporation of glycerol (10 wt %) to the aqueous sol prior to gelation (sample 4 in Table 1) preserves rather well the integrity of encapsulated bacteria, and links to the matrix are hardly observed, even 6 days after encapsulation.

In our previous work on cell viability,[11c] we proposed a similar approach through the encapsulation of living cells in hybrid organic−inorganic matrixes prepared from an organically modified alkoxysilane precursor such as glycidoxypropyltrimethoxysilane (GPTMS) and poly(ethylene glycol) as a dopant. Our belief was that this matrix could provide even better viabilities than Livage's host matrix because of the presence of an additional organic moiety (e.g., glycidoxypropyl groups) covalently attached to the silica network. The experimental data obtained showed viabilities better than those of cells encapsulated in TMOS based sol−gel materials but worse than those of cells suspended in a buffered solution.[11c] The partial success in preserving the active bacteria should be most likely due to the poor hydrophilic nature of glycidoxypropyl groups, which makes unlikely their mutual attraction with bacteria, hence, limiting their ability to protect bacteria from the silanol groups to just their bulky character. Furthermore, we have now observed that the biocompatibility of GIE (with a molecular structure quite similar to that of the glycidoxypropyl groups pending from GPTMS) is poor, and bacteria growth is completely disrupted for weight percents above 0.75% (Figure 2B).

Thus, in this work we have tested the organically modified siloxane precursor GLTES, an alkoxide precursor recently described by Brennan and co-workers.[19] GLTES has shown an excellent ability to preserve enzymatic activity, but there is no data in regards to its compatibility with *E. coli*. To address this issue, we have studied the exponential growth of *E. coli* in a growth medium containing GLTES concentrations of up to 10 wt %. Growth is completely disrupted in the presence of 10 wt % GLTES (Figure 2C). However, reduction of GLTES to 7 wt % retards, but does not impede, cell growth, suggesting that bacteria can adapt to the presence of moderate concentrations of GLTES. At the GLTES concentrations used for biocomposites (e.g., 3.8 wt %), growth retardation is quite small. These results are promising for the achievement of a highly biocompatible biocomposite to host bacteria based on GLTES/TEOS.

The viability of cells encapsulated in GLTES/TEOS was corroborated by fluorescence. In this case, the hydrophilic character of the gluconamide moiety makes necessary more than 6 days for DCPK diffusion through the gel and induction

(18) Zhang, Y.; Wang, S.; Eghtedari, M.; Motademi, M.; Kotov, N. A. *Adv. Funct. Mater.* **2005**, *15* (5), 725.
(19) Cruz-Aguado, J.; Chen, Y.; Zhang, Z.; Elowe, N. H.; Brook, M. A.; Brennan, J. D. *J. Am. Chem. Soc.* **2004**, *126*, 6878.

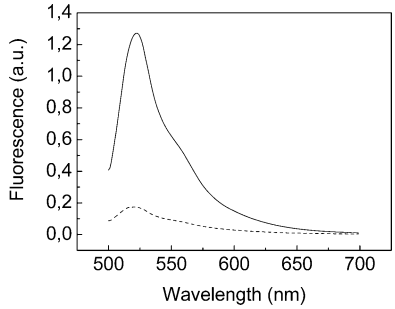

Figure 6. Fluorescence response of *E. coli*-GFP cells grown in the absence of DCPK and induced with a glycerol/water solution of DCPK 6 days after encapsulation in a TEOS based silica gel (sample 2, dashed line) and in a GLTES/TEOS based silica gel (sample 5, solid line).

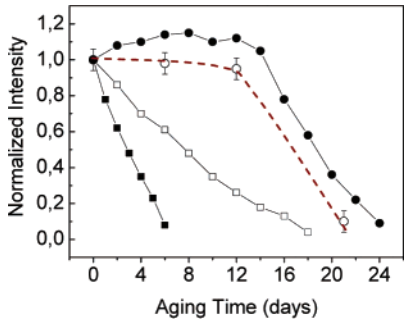

Figure 7. Normalized fluorescence intensity reached for *E. coli*-GFP encapsulated in GLTES/TEOS based silica gels (○) in comparison with data obtained in ref 11c for suspended (●) and encapsulated in TMOS (■) and GPTMS/TMOS based silica gels (□).

of fluorescence response. Under these circumstances and to avoid undesirable sample aging during the induction process, samples (GLTES/TEOS and also TEOS based for comparison) were induced with a water solution of DCPK containing also glycerol (10 wt %). To ensure that glycerol does not interfere the induction process, a TEOS based biocomposite was also induced in a water solution of DCPK free of glycerol. The response of TEOS based biocomposites against DCPK was similar whether water or water/glycerol solutions were used. The number of living cells 6 days after encapsulation in GLTES based biocomposites was remarkable, significantly larger than in TEOS based biocomposites (Figure 6). Actually, bacteria viability in GLTES/TEOS based biocomposites was in a range similar to that of bacteria suspended in buffered solution (Figure 7) thanks to the chemical barrier provided by the gluconolactone groups, which allows for efficient bacteria isolation from the silica porous surface. After ∼22 days, both suspended and encapsulated bacteria no longer showed metabolic activity.

Cryo-SEM analysis of the GLTES/TEOS biocomposites aged for 6 days showed bacteria that look very much like the metabolically active nonaged bacteria encapsulated in alcohol-free silica matrixes (compare Figure 3F,B). This again confirms the lack of toxicity of the biocomposites prepared in this work. In this case, the sugarlike composition of the organic moiety pending from the porous surface of the resulting host matrix is more similar to that of the polysaccharides of the bacterial outer membrane[17] than that of the glycidoxypropyl groups used in our previous work. Furthermore, the bulkier character of gluconamide than that of the glycidoxypropyl groups must also help to provide a more efficient isolation of the cell membrane from the silanol groups. Finally, besides biocompatibility and sterical hindrance, gluconamide groups are capable of establishing favorable hydrophilic interactions with *E. coli*, which definitively keeps bacteria away from silanol groups. Encapsulated bacteria are indeed dead 22 days after encapsulation, but absence of nutrients rather than host matrix interactions seems to be the most plausible cause of death (see Supporting Information).

Conclusions

Cryo-SEM has been shown to be very useful for the analysis of living cells encapsulated in hydrated sol−gel materials, given that it provides a map of the water distribution within the host matrix. Analysis of the viability of encapsulated cells combining fluorescence-based determination of their metabolic activity and in situ visualization of cells by cryo-SEM has provided unique evidence about how deleterious for membrane integrity is the use of nonaqueous encapsulation routes. Damage of the cell envelope and irreversible loss of bacteria activity seem also to occur during aging upon bacteria exposure to silanol groups located at the surrounding host matrix. Moreover, cryo-SEM suggests that bacteria isolation from the porous silica surface would result in more efficient membrane preservation. On the basis of this information, we have been able to manage the required conditions for the preparation of a highly biocompatible host matrix (e.g., GLTES/TEOS based biocomposites). The chemical barrier provided by gluconolactone groups allows for bacteria viabilities in a range similar to those observed for bacteria suspended in a buffered solution and much higher than those found for purely silica based biocomposites. In good concordance with cryo-SEM suggestions, the presence of the barrier isolates encapsulated bacteria from the silica surface and considerably prolongs their life span. This feature will now allow focusing future analyses on the possible beneficial role of the presence of nutrients within the matrix to prolong cell viability even longer.

Acknowledgment. The authors thank Fundación Domingo Martínez, MEC (Grant BMC2003-00063), and CSIC (Grant 200460F027) for financial support. M.L.F. also thanks MEC for a Ramon y Cajal research contract. Prof. Reyes Mateo is acknowledged for valuable support with fluorescent experiments. Prof. Carmen Ascaso and Fernando Pinto are acknowledged for fruitful discussions and assistance with cryo-SEM experiments. TPA, Inc., is acknowledged for valuable support.

Supporting Information Available: Fluorescence response of *E. coli*-GFP cells encapsulated in a TMOS based biocomposite and suspended in a buffered solution and cryo-SEM micrographs of a biocomposite aged for 24 hours at 4 °C in air and of a biocomposite wet aged in a buffered solution for 22 days (PDF). This material is available free of charge via the Internet at http://pubs.acs.org.

CM0522275